

## STEADY-STATE AND DYNAMIC SIMULATION OF CRUDE OIL DISTILLATION USING ASPEN PLUS AND ASPEN DYNAMICS

Juma Haydary, Tomáš Pavlík

*Institute of Chemical and Environmental Engineering, Faculty of Chemical and Food Technology, Slovak University of Technology, Radlinského 9, 812 37 Bratislava, e. mail: [juma.haydary@stuba.sk](mailto:juma.haydary@stuba.sk)*

Received February 4, 2009, accepted April 15, 2009

---

### Abstract

Steady-state and dynamic simulation of Preflash and Atmospheric column (Pipestill) in a real crude oil distillation plant was performed using ASPEN simulations. Steady-state simulation results obtained by ASPEN plus were compared to real experimental data. Experimental ASTM D86 curves of different products were compared to those obtained by simulations. Influence of the steam flow rate in the side strippers and of the heat flow removed in pumparounds was analyzed. Significant influence of the heat flow removed in pumparounds on the flow conditions in the column and on the product composition is explained.

Steady-state flowsheet was completed by dynamic simulation requirements and exported to ASPEN Dynamics for simulations in dynamic mode. The behavior of the products flow rate in dynamic regime was observed after changing the crude oil feed by 10%. Two different control methods based on composition (ASTM D86 95% boiling point) and temperature at the second stage were applied in dynamic simulation. The time needed to reach a new steady-state, deviation, and ability of reaching the preset parameters of both methods were compared.

**Key words:** crude oil distillation, simulation, ASPEN.

---

### 1. Introduction

Optimization of the crude oil separation process becomes increasingly important because of the high energy costs and ecological requirements for quality oil products. Computer simulation is one of the most important steps of process optimization. However, due to complex composition of oil and complex design of oil fractionators, simulation of oil distillation requires a specific approach.

Crude oil is a mixture of many thousands of components varying from light hydrocarbons such as methane, ethane, etc., to very high molecular weight components. The composition of crude oil depends also on the location of exploitation. These facts exclude the use of classical characterization methods for the crude oil composition by mole or mass fractions of individual components. In petroleum refining, the boiling point ranges are used instead of mass or mole fractions. Three types of boiling point analysis are known: ASTM D86, ASTM D158 and TBP (true boiling point). Properties of a petroleum stream are not specified in terms of composition. Instead, properties such as 5 % point, 95% point, final boiling point, flashpoint and octane number are used.

The method for quantitative calculations of the petroleum fractions is to break them into pseudocomponents. Each pseudocomponent has its average boiling point, specific gravity, and molecular weight.

For steady-state simulations of petroleum processes, ASPEN Technologies provides the tool ASPEN Plus Petroleum. After process simulation in the steady-state regime, ASPEN Dynamics can be used for the dynamic simulation of the process.

The dynamic simulation of such a system enables the understanding of its behavior after changing an input parameter. In a crude oil distillation plant, the system behavior

can be affected by the dynamics of individual sub-processes. Due to this fact, a rigorous and complete simulation of the system is required. Process control and safety analysis are the two main areas of using dynamic simulations.

The aim of this work was to apply ASPEN Plus and ASPEN Dynamics in steady-state and dynamic simulations of Preflash and Atmospheric columns in a crude oil distillation plant, and to compare the steady-state simulation results with real measured data.

## 2. Mathematical model and process simulation

For mathematical description of a distillation process in refining columns, the theoretical stage method is usually used. The number of theoretical stages of an existing column is estimated by multiplication of the real number of stages and column efficiency. For each theoretical stage, the mass balance of individual components or pseudocomponents, enthalpy balance, and vapor liquid equilibrium equation can be written. The sum of these equations creates the mathematical model of a theoretical stage. The mathematical model of a column is composed of models of individual theoretical stages.

### 2.1 Mass balance

Figure 1 represents the general scheme of a stage.

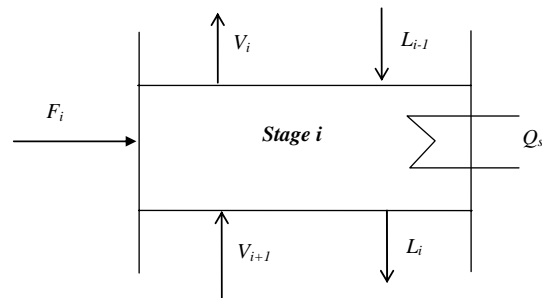


Figure1: Scheme of a column stage

Steady-state mass balance of stage  $i$  and component  $j$  can be describe by:

$$L_{i-1}x_{i-1,j} + V_{i+1}y_{i+1,j} + F_i f_{i,j} - L_{i,j}x_{i,j} - V_i y_{i,j} = 0 \quad (1)$$

where  $V_i$  is the mole flow of vapors from stage  $i$ ,  $V_{i+1}$  is the mole flow of vapors entering the stage,  $L_i$  is the mole flow of liquid from stage  $i$ ,  $L_{i-1}$  is the mole flow of liquid entering the stage,  $x$ ,  $y$  and  $f$  represent the mole fractions in liquid, vapor and feed, respectively.

In the dynamic regime, the right side of equation (1) does not equal zero, but represents accumulation of mass on the stage.

$$L_{i-1}x_{i-1,j} + V_{i+1}y_{i+1,j} + F_i f_{i,j} - L_{i,j}x_{i,j} - V_i y_{i,j} = \frac{d(W_i x_{i,j})}{d\theta} \quad (2)$$

where  $W_i$  represents the liquid holdup on the stage. The holdup of the vapor phase is negligible at the pressures lower than 10 atm, when it is less than 20% of the liquid holdup<sup>[1]</sup>.

The liquid holdup on the stage can be calculated as:

$$W_i = \rho_{Li} A_{Ti} h_{Ti} + \rho_{Li} A_{Di} h_{Di} \quad (3)$$

where  $\rho_{Li}$  is the liquid density at stage  $i$ ,  $A_{Ti}$  is the active surface area of the stage,  $A_{Di}$  is the surface area of the downcorner,  $h_{Ti}$  is the liquid height on the stage and  $h_{Di}$  is the liquid height in the downcorner.

The Francis equation can be used to calculate the liquid mole flow from stage  $i$ <sup>[2]</sup>:

$$L_i = c\sqrt{2gl_{wi}\rho_{Li}}(h_{Ti} - h_{wi})^{1.5} \quad (4)$$

where  $c$  is a constant with the value of about 0.42,  $l_{wi}$  is the weir length,  $h_{wi}$  is the weir height.

## 2.2 Enthalpy balance

For stage  $i$  and the steady-state, it can be written:

$$L_{i-1}h_{i-1} + V_{i+1}h_{i+1} + F_i h_{Fi} - L_i h_i - V_i h_i + Q_M - Q_s - Q_{loss} = 0 \quad (5)$$

$h_i$ ,  $h_{i+1}$ ,  $h_{i-1}$  and  $h_{Fi}$  are the molar enthalpies of corresponding streams,  $Q_M$  is the heat of mixing,  $Q_s$  represents the external heat source and  $Q_{loss}$  represents the heat losses.

In case of the dynamic regime, the right side represents the heat accumulation on stage  $i$ .

$$L_{i-1}h_{i-1} + V_{i+1}h_{i+1} + F_i h_{Fi} - L_i h_i - V_i h_i + Q_M - Q_s - Q_{loss} = \frac{d(W_i h_i)}{d\theta} \quad (6)$$

To calculate enthalpy, the Lee-Kessler correlation<sup>[3]</sup> can be used.

## 2.3 Vapor-liquid equilibrium

For a theoretical stage, an equilibrium state between the vapor and liquid phases was assumed. The general equilibrium equation has the form:

$$y_j = K_j x_j \quad (7)$$

where  $K_j$  is the equilibrium coefficient for component  $j$ .

The selection of a thermodynamic method for the calculation of the equilibrium coefficient is the most important step for the simulation accuracy. Aspen plus provides a number of thermodynamic models. Suitable models for refining applications can be divided into two groups; the first group based on the state equation of gases is suitable for real components. The PR (Peng-Robinson) state equation and RKS (Redlich-Kwong-Soave) state equation are examples from this group. The second group developed especially for hydrocarbon mixtures is suitable mainly for the pseudocomponents. Braun K10, Chao-Seader and Grayson-Streed are examples of these models.

Braun K10 is a model suitable for mixtures of heavier hydrocarbons at pressures under 700 kPa and temperatures from 170°C to 430°C. The values of K10 can be obtained by the Braun convergence pressure method using tabulated parameters for 70 hydrocarbons and light gases.

The Chao-Seader model in Aspen-Plus<sup>[4]</sup> uses the Chao-Seader correlation for the calculation of fugacity coefficient of pure components in liquid phase ( $v_j^0$ ), Scatchard-Hildebrand model for activity coefficients ( $\gamma_j$ ), Redlich-Kwong state equation for fugacity coefficient of the vapor phase  $\Phi_i$ <sup>[5]</sup> and the Lee-Kesler correlation for calculation of enthalpy<sup>[3]</sup>.

The equilibrium coefficient  $K_j$  is then calculated as:

$$K_j = \frac{v_j^0 \gamma_j}{\Phi_i} \quad (8)$$

The model provides optimal results at temperatures from -70°C to 260°C and pressures less than 140°C.

The works<sup>[4]</sup> and<sup>[6]</sup> provide instructions for choosing the right method for Aspen simulation.

## 2.4: Input data and oil characterization

A simulation of two columns of a crude oil distillation plant is the object of this work. The first column was the Preflash column which is a relatively simple column with one feed, a partial condenser and a reboiler. The second column was a more complex, atmospheric, with three steam strippers and three pumparounds.

The feed of 350 tons/hr of crude oil entered the bottom stage of the Preflash column with 11 theoretical stages. The pressure in the column was 2.5-3 atm.

The product flows of the Preflash column were set as in Table 1:

Table 1: Mass flows of the preflash column products

Product	Mass flow (ton.hr <sup>-1</sup> )
Lights	1.4
Light naphtha	23.8
Bottoms- feed to atmospheric column	325

The bottoms of the Preflash column was preheated to 350°C in a furnace before entering the atmospheric column. The atmospheric unit was a column with the separation ability of 24 theoretical stages. The real column did not have a condenser; the condenser in the real column was substituted by a pumparound returning the liquid to the first stage. Steady-state simulation in ASPEN Plus enables the simulation of a column without a condenser, but for a stable dynamic simulation in ASPEN Dynamics, a column model with a partial condenser without liquid distillate was used. Beside the distillate (heavy naphtha) and bottoms (feed to the vacuum column), three products were removed via side steam strippers. The mass flows of atmospheric unit products are shown in Table 2.

Table 2: Mass flows of the Atmospheric column products

Product	Mass flow (ton.hr <sup>-1</sup> )
Heavy naphtha	48.9
Kerosene	36
Light gas oil (LGO)	76
Heavy gas oil (HGO)	38.9
Atmospheric residue	149.2

The oil was characterized by the TBP curve, specific gravity and light component analysis. Figure 2 shows the input of TBP data into ASPEN Plus. The ASTM D86 curves and specific gravity of individual products for comparison of the simulation results and the real measured data were available.

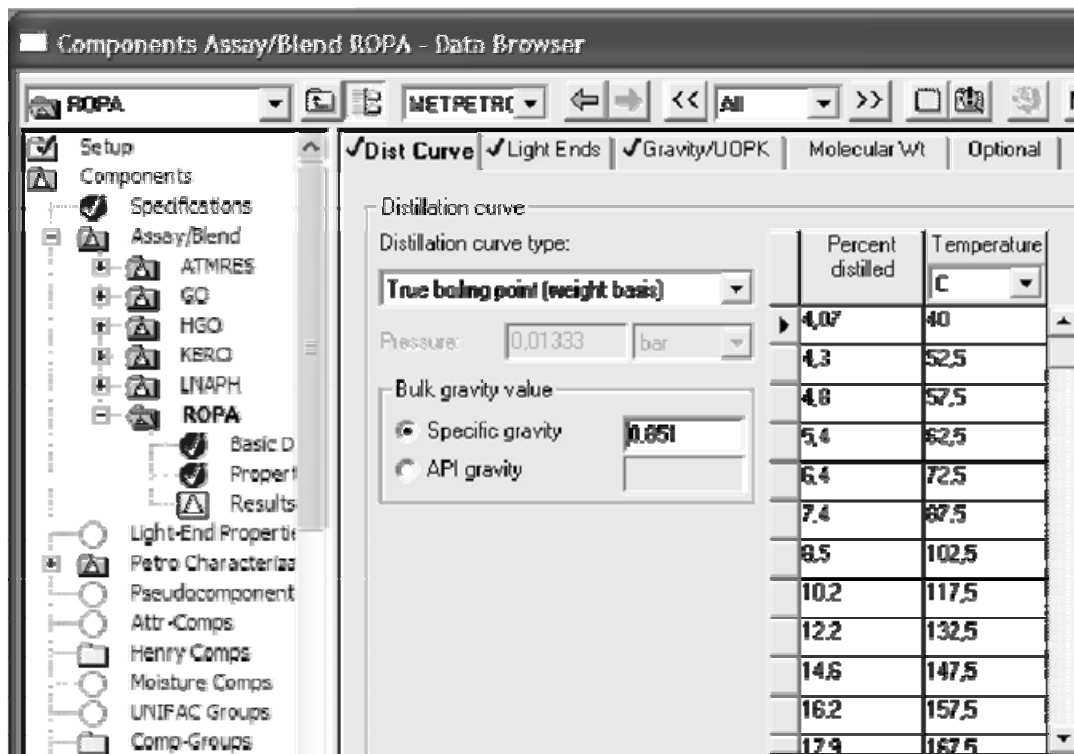


Figure 2: Input of TBP curve into ASPEN Plus



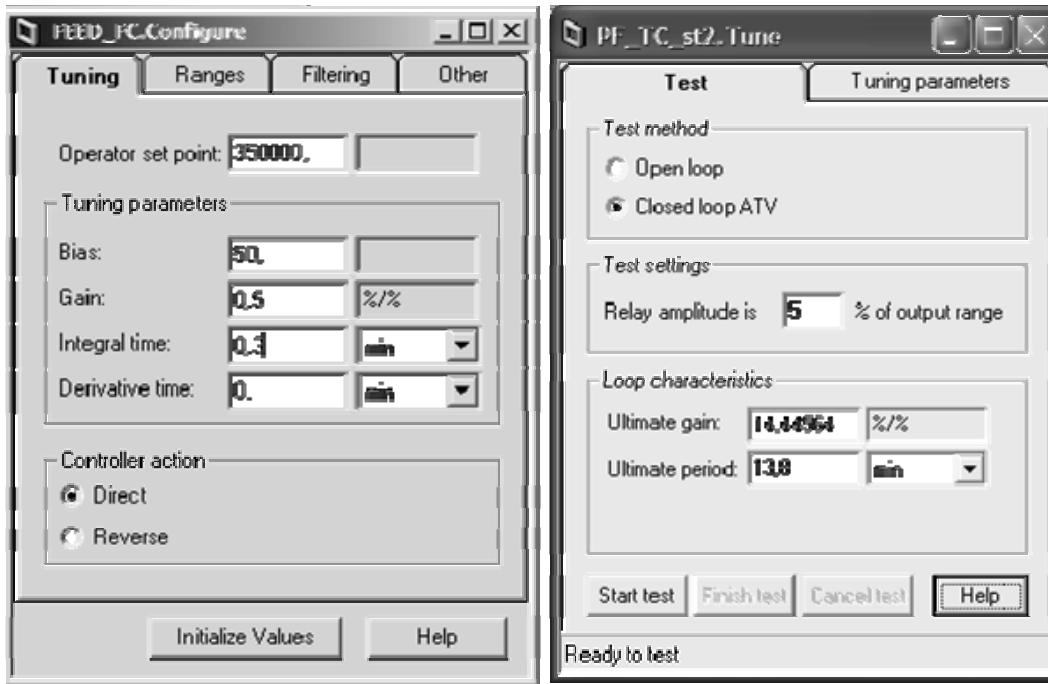


Figure 4: Controller parameters setting

### 3. Results and discussion

#### 3.1 Steady state simulation results

Experimental ASTM D86 or TBP data of all products for comparison with the simulation results were available. Flow rate of the products and other process conditions were set as in a real process. Figure 5 shows the ASTM D86 curve for the liquid distillate of the Preflesh column (Light naphtha). Generally, simulation results are in quite good agreement with the experimental data. However, the first part of the curve, corresponding to light components, shows better conformity between the simulation and experiment.

Figures 6-9 show a comparison of the simulated ASTM D86 curve respectively the TBP curve with the experimental data for products of the Atmospheric columns. The best agreement was observed for the TBP curve of the atmospheric column bottoms product. ASTM D86 curves of other products showed greater differences between the simulation and experimental data. However, the maximum difference was around 10°C.

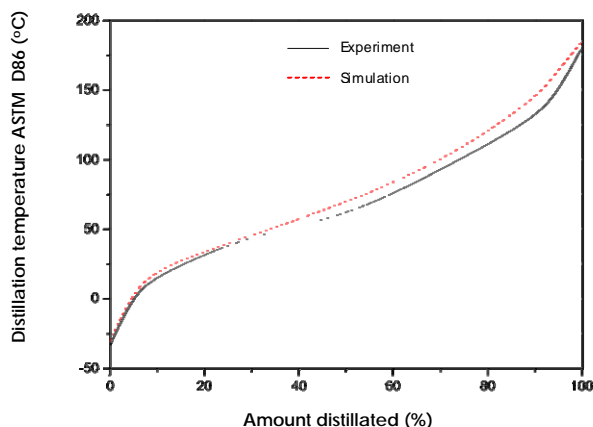


Figure 5: Simulated and experimental ASTM D86 curves of Light naphtha

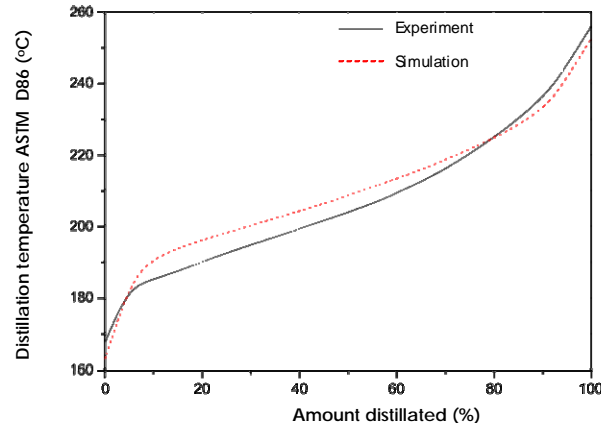


Figure 6: Simulated and experimental ASTM D86 curves of Kerosene

The influence of stripping steam flow rate on the temperature of ASTM D86 5% and 95% of products from side strippers was analyzed. By changing the flow rate of the stripping steam by  $\pm 50\%$ , the temperature of ASTM D86 5% changed by about 2-3°C.

However, the influence of this parameter on the temperature of ASTM D86 95 % was practically negligible. Figure 10 shows an example of such analysis for kerosene. The results show that the flow rates in the side strippers do not affect the quality of the products significantly.

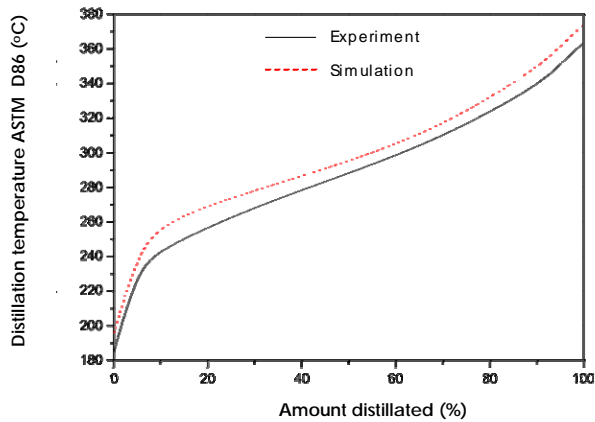


Figure 7: Simulated and experimental ASTM D86 curves of Light gas oil (LGO)

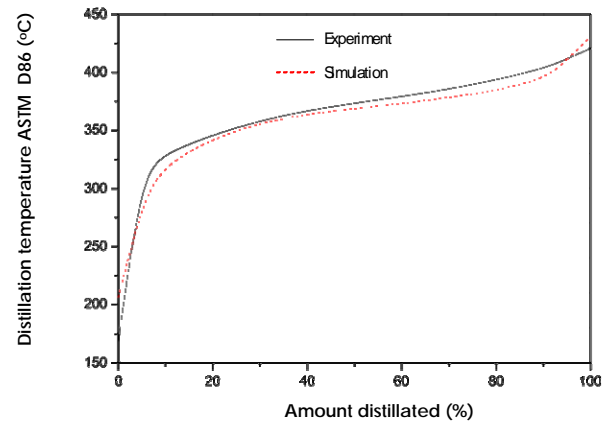


Figure 8: Simulated and experimental ASTM D86 curves of Heavy gas oil (HGO)

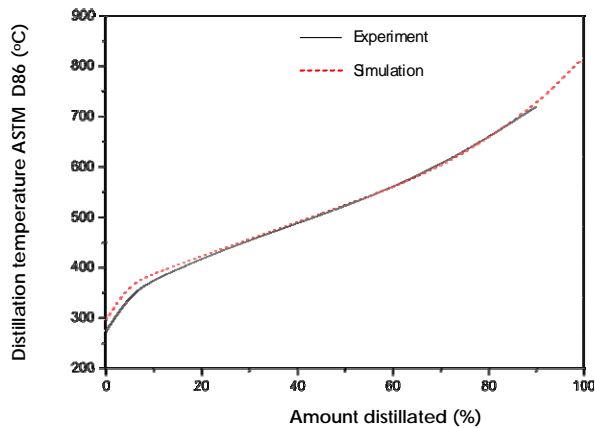


Figure 9: Simulated and experimental TBP curves of atmospheric residue

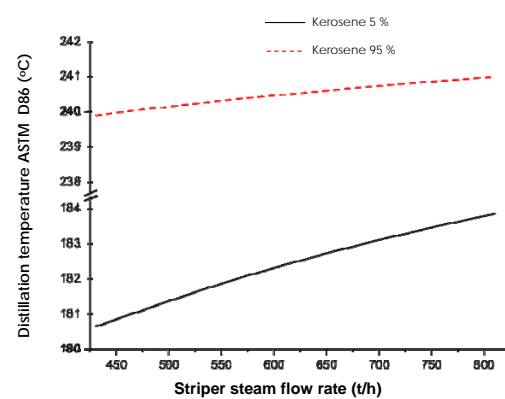


Figure 10: Influence of stripper steam flow rate on kerosene composition

Another analysis procedure considers the influence of the amount of heat removed in pumparounds. In case of pumparound 1 near the head of the column, the amount of heat removed was changed by  $\pm 20\%$ . Figures 11 and 12 show the influence of this parameter on the profile of liquid and vapor flow, respectively, in the column. Increasing the removed heat flow by 20%, the liquid mass flow on the stages increased by about 35%. Figure 13 shows the influence of the heat flow removed in pumparound 1 on the temperature profile in the column.

Removing more heat in pumparound 1 decreases the temperature of the liquid returning to the column. Lower temperature of the returned liquid causes additional condensation of vapors and the flow rate of the liquid phase increases. At the same time, it causes condensation of lighter components. Liquid flowing down in the column contains more light components. This results in the achievement of liquid-vapor equilibrium at lower temperatures. Because of the facts described above, the amount of heat removed in the pumparounds has a crucial effect on the temperature on the stages. The effect on temperature decreases downwards from the stage onto which the liquid is returned. The temperature of stages above this stage is practically unaffected.

The degree of separation of two neighboring products is given by the difference between the temperature of ASTM D86 95% of the lighter and 5% of the heavier product. If the temperature of ASTM D86 5% of the heavier product is higher than the

temperature of ASTM D86 95% of the lighter product it means that a gap area exist. If the situation is reversed, it represents an overlap area.

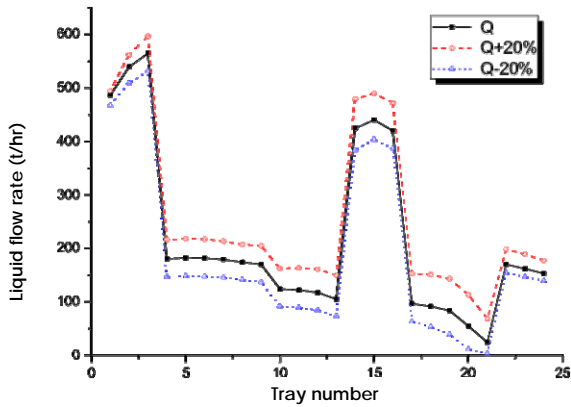


Figure 11: Influence of heat flow removed in Pumparound 1 on the liquid flow rate in the atmospheric column

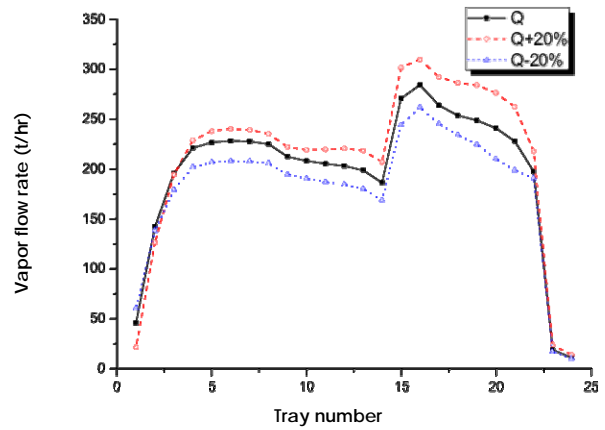


Figure 12: Influence of heat flow removed in Pumparound 1 on the vapor flow rate in the atmospheric column

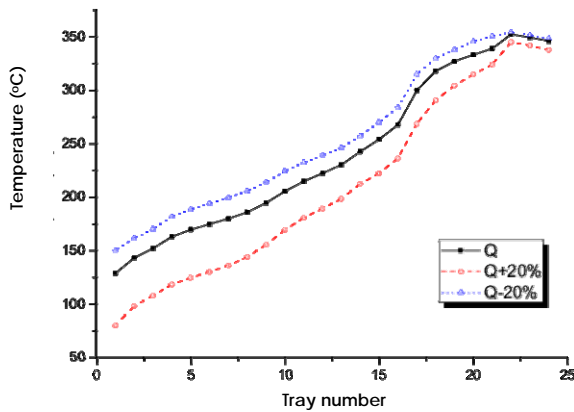


Figure 13: Temperature profile of atmospheric column at different heat flow rates removed in Pumparound 1

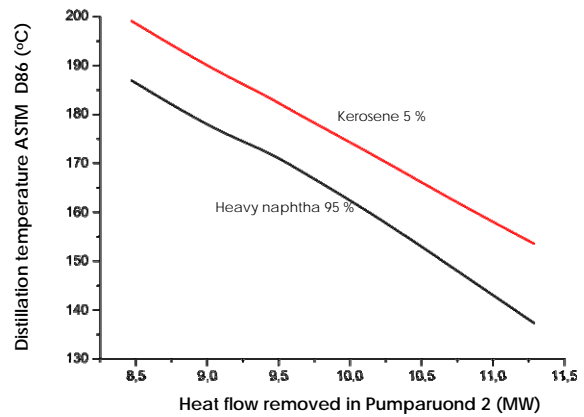


Figure 14: Influence of heat flow removed in Pumparound 2 on the degree of Kerosene and Heavy naphtha separation

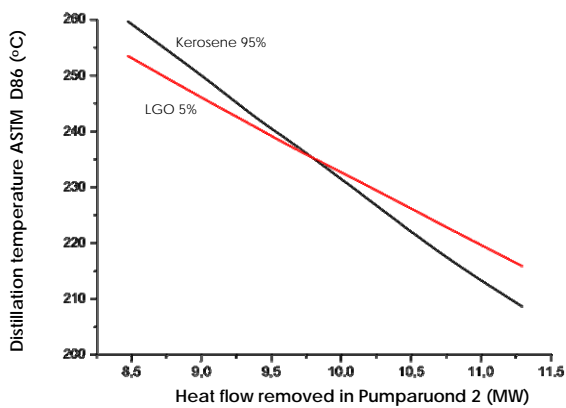


Figure 15: Influence of heat flow removed in Pumparound 2 on the degree of LGO 5% and Kerosene 95% separation

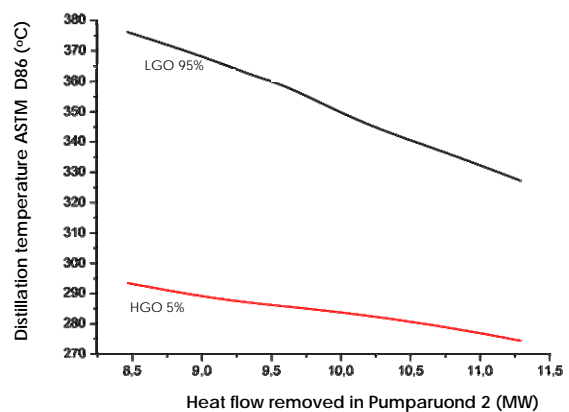


Figure 16: Influence of heat flow removed in Pumparound 2 on the degree of HGO 5% and LGO 95% separation

On Figures 14-16 the influence of heat amount removed in pumparound 2 on the degree of separation of different neighboring pair of products is shown. Kerosene and heavy naphtha (Figure 14) show a gap area which is only slightly changed by increasing of the heat removed in the pumparound; however, the situation is different in case of

LGO and Kerosene (Figure 15), where the degree of separation firstly shows an overlap area, then, after showing a cross point, a gap area is created between the ASTM D86 95% boiling point of the light product and ASTM D86 5% boiling point of the heavy product. The degree of HGO and LGO separation (Figure 16) shows an overlap area which decreases by increasing the heat flow removed.

Removing more heat in pumparounds generally affects the separation process positively; however, the amount of heat removed in pumparounds is often limited due to other process or construction characteristics of the system.

### 3.2 Dynamic simulation results

The products mass flow was observed after increasing the feed flow of crude oil by 10%. Two types of control were used and compared. In the first case, mass flow of the products was changed until the composition (ASTM D86 95 % boiling point) reached the value corresponding to the given product. In the second method, the flow rate of the given product was changed until the temperature at the second stage reached a specified value.

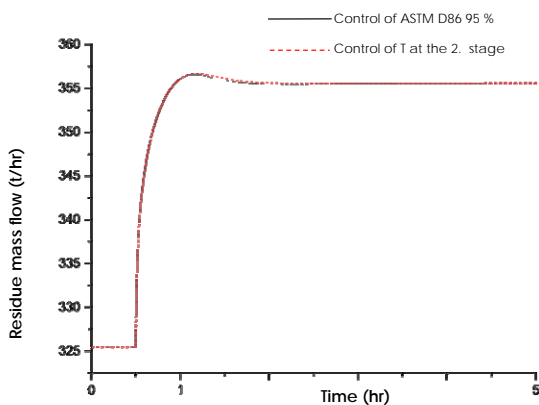


Figure 17: Behavior of the Preflash column residue flow rate after increasing the crude oil feed flow rate by 10%

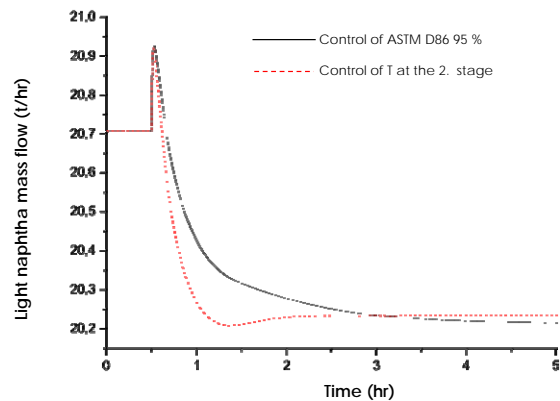


Figure 18: Behavior of the Preflash column liquid distillate (light naphtha) flow rate after increasing the crude oil feed flow rate by 10%

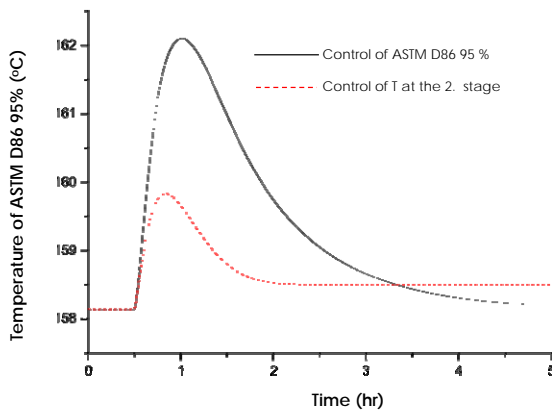


Figure 19: Comparison of different control methods, behavior of Preflash column liquid distillate composition

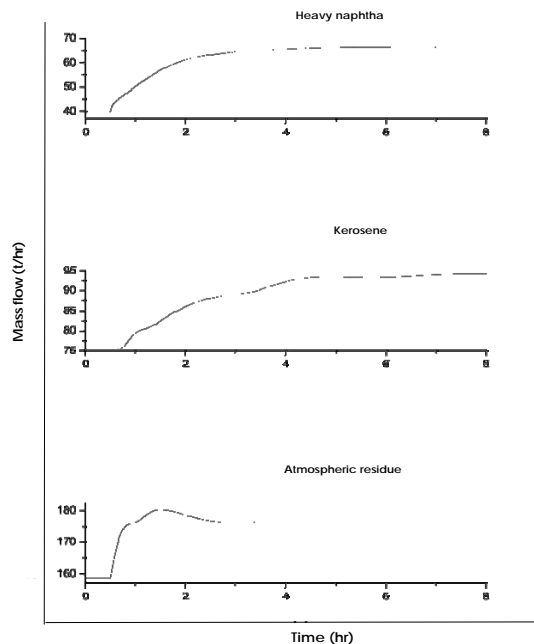


Figure 20: Flow rate behavior of products of atmospheric column after increasing the crude oil feed flow rate by 10%

Figures 19 and 20 show the behavior of the Preflash column product after increasing the feed flow by 10%. Figure 19 shows the comparison of the Preflash column liquid distillate composition when different control methods were used. Increasing the mass flow of the feed by 10%, the mass flow of the residue and lights reached a new steady-state at higher rate flows; however, the mass flow of Light Naphtna (liquid distillate from the Preflash column) unexpectedly, although slightly, decreased.

The control method using temperature at the second stage was much faster than the control by composition (ASTM D86 95% boiling point). The time necessary to reach a new steady-state by the second stage temperature control was 1.5 hr compared to 4.5 hr by the composition control. Also, deviation of the first mentioned method was significantly lower than that of the second method. However, as it results from Figure 19, composition of the product is slightly different.

Figure 20 shows the flow rate behavior of some products of the atmospheric column (Pipestill) using ASTM D86 95% boiling point control. The time needed to achieve a new steady-state was from 2.5 hr for the atmospheric residue to 4.5 hr for kerosene. Experimental data for the simulation results verification in dynamic mode were not available. Some limitation of ASPEN Dynamics in supporting different types of column configurations and in dynamic simulation of the process start were found.

#### 4. Conclusion

ASPEN Plus and ASPEN Dynamics enable the simulation of very complex distillation systems such as petroleum fractionators. Steady-state simulation results were in good agreement with experimental data. From the analysis of side steam strippers results that deviations of the steam flow rate do not influence the products composition significantly. The value of heat flow removed in pumparounds affects the products composition significantly. Increase of the heat flow removed in pumparounds has a positive influence on the distillation process.

Dynamic simulation of very complex systems such as Pipestill is possible by ASPEN Dynamics. However, for successful dynamic simulation, detail properties of the system, careful setting of controller parameters and long calculation time are required.

In supporting different column configurations and process start, some limitation of ASPEN Dynamics were observed. Control of the product composition (ASTM D86 95% boiling point) can be replaced by control of the temperature at the second stage. This control method requires shorter time to reach a new steady-state and shows smaller deviation; however, a small difference in the product composition was observed.

#### References

- [1] Skogestad, S.: Dynamics and Control of Distillation Columns – a critical survey, Modeling, Identification and Control, 18, 177-217, 1997.
- [2] Pesier, A.M., Grover, S. S. : Dynamic Simulation of a Distillation Tower, Chemical Engineering Progress, 58 (9), 65-70, 1962.
- [3] Lee, B.I., Kesler, M.G. : A generalized thermodynamic correlation based on three-parameter corresponding states, AIChE Journal, 21 (3), 510-527, 1975.
- [4] Aspen Physical Property System, Physical property methods and models, Aspen Technology, 2001.
- [5] Chao, K.C., Seader, J.D. : A General Correlation of Vapor-liquid Equilibria in Hydrocarbon Mixtures, AIChE Journal, 7 (4), 598-604, 1961.
- [6] Carlson, Eric C.: Don't gamble with physical properties for simulations, Chemical Engineering Progress, 92 (10), 35-46, 1996.
- [7] Luyben, William L. : Distillation Design and Control Using Aspen Simulation, John Wiley & Sons, New York, 2006.